

Toward Recyclable Polymers: Ring-Opening Polymerization Enthalpy from First-Principles

Huan Tran, Aubrey Toland, Kellie Stellmach, McKinley K. Paul, Will Gutekunst, and Rampi Ramprasad*



Cite This: *J. Phys. Chem. Lett.* 2022, 13, 4778–4785



Read Online

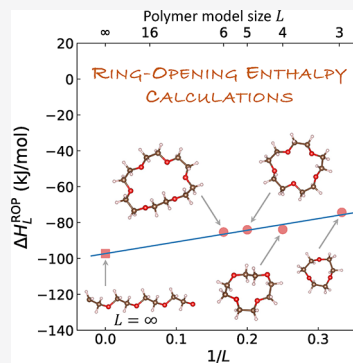
ACCESS |

Metrics & More

Article Recommendations

Supporting Information

ABSTRACT: Ring-opening polymerization (ROP) enthalpy ΔH^{ROP} is an important thermodynamic property controlling the polymerization of cyclic monomers. While ΔH^{ROP} can be measured, computing ΔH^{ROP} for realistic polymer systems with an error of $\approx 5\text{--}10 \text{ kJ/mol}$ is critical for designing new monomer systems for depolymerizable polymers. We have developed a first-principles computational scheme in which multiple challenges in computing ΔH^{ROP} are resolved definitively including extensive exploration of conformational states and adequately addressing finite size effects. This scheme is validated on a diverse benchmark set of 42 ROP polymers for which reliable experimental values of ΔH^{ROP} are available. For this set, the ΔH^{ROP} root-mean-square error is $\approx 7 \text{ kJ/mol}$, about 3-times smaller than conventional approaches. This development opens up new pathways to build up a high-quality database of ΔH^{ROP} for downstream predictive machine-learning models and ultimately to accelerate the design of depolymerizable polymers with desired properties.



Polymers appear in every corner of the world. From daily packaging materials to essential constituents of high-tech equipment, materials from this class are profoundly impacting our lives.^{1,2} The superior chemical and thermodynamic stability of polymers, for example, plastics, make them extremely difficult to recycle when they reach their end-of-life. About 75% of postconsumer-waste plastics, or roughly 27 million tons, ended up in the environment in 2018.³ Plastics pollution has thus become a global challenge.^{4–12}

Among many methods adopted to recycle polymers that have reached their end-of-life, an effective approach is to transform (or depolymerize) the polymer waste back to monomers before purifying and repolymerizing them.^{8–11} This chemical recycling to monomer method is preferable when other conventional methods, for example, mechanical recycling, can no longer be used. This method also has inherent advantages to mechanical recycling since materials with the exact same properties can be regenerated (traditional recycling frequently leads to polymer chain degradation with deteriorated mechanical properties). A fundamental challenge of this chemical recycling method is that not all polymers can be (efficiently) depolymerized. One class of polymers, that is, those created by opening cyclic monomers, stands out because they are, in principle, depolymerizable.^{8,13–15} Therefore, such a ring-opening polymerization (ROP) process is a timely topic of research and development in the context of sustainability.^{8,13–17}

The thermodynamics of polymerization is described by the Gibbs free energy $\Delta G \equiv \Delta H - T\Delta S$, where T is the temperature, while ΔH and ΔS are the polymerization enthalpy and entropy, respectively.¹⁸ For the polymers of interest here, both ΔH and ΔS are negative; thus, $\Delta G < 0$

when $T < T_c$, a critical value defined as the ceiling temperature.¹⁹ Below T_c , polymerization is favored, while above T_c , thermodynamics favors depolymerization. At ambient temperatures and below, and for most conventional ROP involving small cyclic monomers (about six-membered and below), the driving force for ROP is the ring strain. If ring strain increases, the ROP enthalpy ΔH^{ROP} becomes more negative, and the monomers will more easily polymerize.^{20,21} While ΔH^{ROP} can be measured experimentally, computing ΔH^{ROP} at a reliable level of accuracy for realistic situations has hitherto remained a challenge, hence impeding our ultimate objective of designing depolymerizable polymers with desired T_c and other properties.

By definition, ΔH^{ROP} is the difference between the energies of the products, that is, polymers, and the reactants, that is, monomers, in a polymerization reaction. While this picture may look straightforward and simple, reaching a predictive level in computing ΔH^{ROP} for realistic situations is nontrivial. The impression of simplicity may come from the only procedure that has been adopted to-date to model ROP in the scientific literature.^{22–27} In this approach, cyclic monomers are opened, and the two dangling bonds are saturated by two suitable end groups derived from neutral molecular initiators, for example, methanol CH_3OH or methanethiol CH_3SH ,

Received: April 5, 2022

Accepted: May 19, 2022

Published: May 25, 2022



so that the reactions are isodesmic, that is, the numbers and types of bonds are conserved. Then the ground-state atomic configurations of the monomer, the “polymer”, that is, the ring-opened capped monomer, and the initiator molecule, are guessed and optimized using first-principles computations. The energies of those species are then used to estimate ΔH^{ROP} . Key assumptions here are (i) each of the species involved can be described by a single atomic configuration, even at nonzero temperatures, and (ii) the capped ring-opened monomer is a good representation of the polymer. This simplified approach leads to an error of at least $\approx 20.0 \text{ kJ/mol}$ in the ΔH^{ROP} regime between -20 and 0 kJ/mol , which is critical for designing depolymerizable polymers. Therefore, it, at best, can only be used for a qualitative understanding but not for guiding experiments.

In this work, we have developed a robust, quantitative, and high-fidelity scheme to compute ΔH^{ROP} , which significantly surpasses past works. In short, the new scheme involves designing realistic extrapolative models of monomers and polymers, starting from which the configuration spaces are extensively sampled using density functional theory (DFT)^{28,29} computations. The scheme is demonstrated for a diverse benchmark set of 42 ROP polymers for which reliable experimental ΔH^{ROP} values are available, covering multiple chemistries, including cycloalkanes, methyl cycloalkanes, cycloalkenes, ethers, lactams, lactones, thiolactones, polyurethanes, and others. The obtained error of ΔH^{ROP} predictions (relative to experiments) is $\approx 7 \text{ kJ/mol}$ of monomer across the benchmark set, about 3-times smaller than previously adopted approaches. We note here that the chemical accuracy corresponds to an error of about 5 kJ/mol . This new development opens up pathways (i) to quantitatively estimate ΔH^{ROP} to guide new chemistry choices for ROP, (ii) to extract chemical guidelines on features that control ΔH^{ROP} , (iii) to build a high-quality uniform ΔH^{ROP} database for downstream machine-learning model development to instantaneously predict ΔH^{ROP} for new ROP chemistries, and (iv) to accelerate the design of depolymerizable polymers with suitable T_c and other desired properties.

Ring-opening polymerization, as illustrated in Figure 1, is a process during which the (cationic, anionic, or radical)

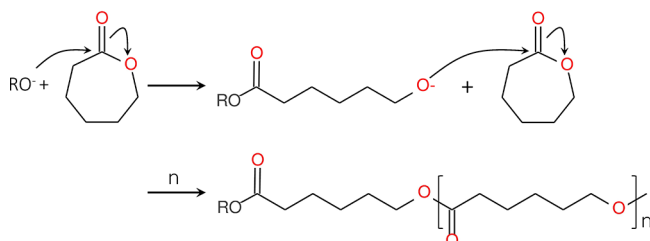


Figure 1. Scheme of a (chain-growth) anionic ring-opening polymerization, in which the anionic group at the end of an initiator or a polymer chain “opens” cyclic monomers and adds them to the chain.³⁰

terminal end group of an initiator or a polymer chain “opens” a cyclic monomer and adds it to the chain.³⁰ In this process, ΔH^{ROP} is a thermodynamic measure of how easy it is to open the rings so that they can be polymerized. A distinctive feature of ROP is the ring strain, largely governed by the ring size, side-chain functional groups, and heteroatoms, which offer critical additional degrees of freedom to control ΔH^{ROP} .

The general trend is that highly strained (small-size) rings are easier to open and polymerization is more favorable.

Reported experimental data of ΔH^{ROP} are highly scattered in the scientific literature, and collecting them is extremely laborious. A carefully curated set of 42 ROP cases, summarized in Figure 2 (detailed information can be found in the

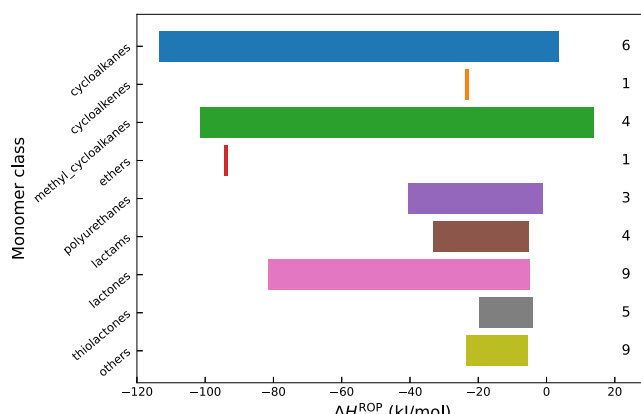


Figure 2. Summary of the experimental data of ΔH^{ROP} used to demonstrate the scheme. For each polymer class, a range of ΔH^{ROP} and number of data points are given in a colored bar and a numbers on the right, respectively.

Supporting Information), was used to validate the computational scheme developed here. Monomers in this benchmark set were categorized into 9 series including cycloalkanes, cycloalkenes, methyl cycloalkanes, ethers, polyurethanes, lactams, lactones, thiolactones, and others. Data for one of these series, that is, thiolactones, were recently produced by us.³¹ Although the regime of ΔH^{ROP} with small magnitude is interesting for the goal of designing depolymerizable polymers, for example, thiolactones, the very wide range of ΔH^{ROP} values, as shown in Figure 2, and the diversity in the chemistry of these series would be a stringent test for our computational scheme.

Figure 2 shows that ΔH^{ROP} for many common ROP reactions is in the range between -20 and 0 kJ/mol . These are very small energy values, considering that 1 kcal/mol , or $\approx 5 \text{ kJ/mol}$, is designated as “chemical accuracy”. Quantitatively predicting such a tiny energy value across diverse chemical spaces is extremely difficult, and it remains a longstanding challenge for computations.^{32–34} In the context of ΔH^{ROP} computations, *ab initio* methods like DFT^{28,29} and beyond must be used.^{22–26} As these methods are computationally expensive, the atomic models adopted thus far are typically small and simple. As mentioned above, cyclic monomers are opened, and the two dangling bonds are saturated by two suitable end groups of a neutral molecular initiator, for example, methanol $\text{CH}_3\text{---OH}$ or methanethiol $\text{CH}_3\text{---SH}$. Then the ground-state atomic configurations of the monomer, the “polymer” (the ring-opened capped monomer), and the initiator molecule are guessed and optimized using first-principles computations. Then ΔH^{ROP} is computed from the energies obtained for those species.

While this approach is practical and intuitive, it has major deficiencies. Modeling each of the species involved in the ROP by a single atomic configuration and representing the polymer by a capped ring-opened monomer (i.e., totally ignoring the macromolecular morphology) led to significant quantitative

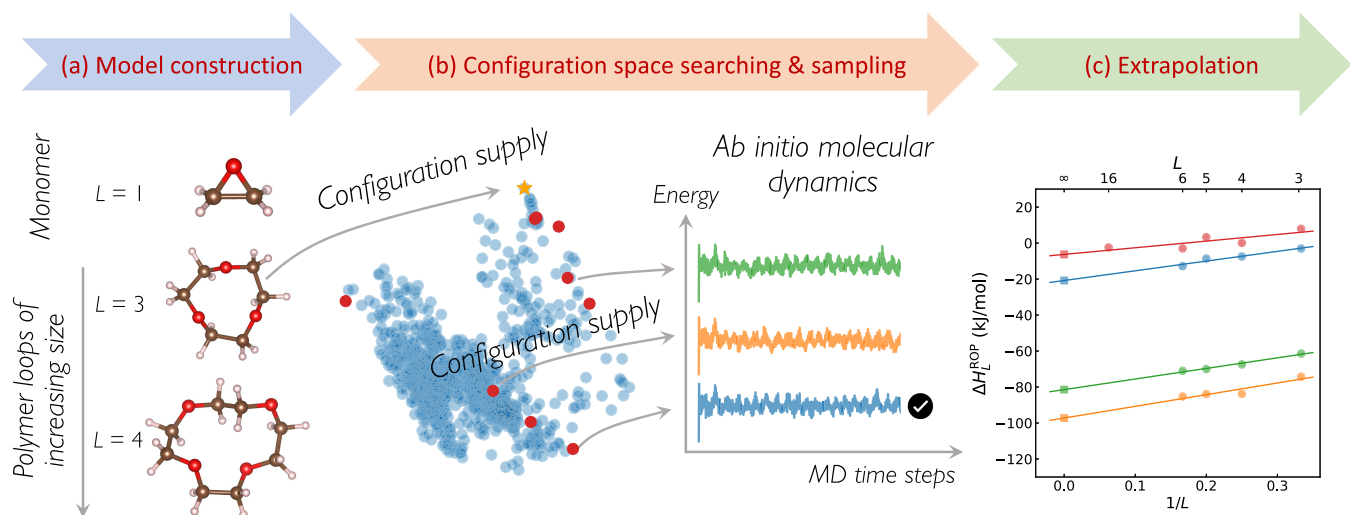


Figure 3. First-principles computational scheme for ΔH_L^{ROP} . In (a) the “model construction” step, atomic configurations of the monomer (with length $L = 1$) and polymer ($L > 1$) are generated. Here, monomer model ($L = 1$) and two polymer models ($L = 3$ and 4) of polyethylene glycol are used for an illustration, in which carbon, oxygen, and hydrogen atoms are given in brown, red, and pink, respectively. Entering (b) the “configuration space searching & sampling” step, the domain corresponding to each configuration is expanded, searched, and sampled using DFT-based molecular dynamics simulations. From the lowest-energy MD trajectory at equilibration (indicated by the check mark), the formation enthalpy ΔH_L^{ROP} of the polymer model of length L is obtained. Within (c) the “extrapolation” step, ΔH_L^{ROP} (given in squares) is determined by extrapolating ΔH_L^{ROP} (given in circles) to the limit of $L \rightarrow \infty$, or equivalently, $1/L \rightarrow 0$.

discrepancies with respect to reality and experiments. This approach ignores the polymer energy spectrum, which is essentially continuous, representing numerous atomic configurations that are very close to the ground state in energy.³⁵ Such strategies have been used mostly for understanding the atomic-level geometric details of the involved species,^{23,24,26} while computed values of ΔH^{ROP} using this approach can, at best, be used to understand trends within a restricted chemical class.^{22,25}

The present scheme, portrayed in Figure 3, was designed to compute ΔH^{ROP} in a more realistic manner. In addition to resolving the aforementioned two assumptions adopted in the present-day approach, effects due to nonzero temperatures are adequately considered. In the first step, a series of atomic models (configurations) of the monomer and polymer are constructed using the Polymer Structure Predictor package.^{35,36} The smallest member of this series, labeled by its size (length) $L = 1$, is an atomic configuration of the monomer itself. Larger members, labeled by $L > 1$ and obtained by multiplying the monomer with several integer values of L to create loops, are used to represent the polymer (Figure 3a). By construction, our models involve no end groups as mentioned above (and thus, no artificial effects from them) while still allowing results computed for the finite-size polymer models ($L > 1$) to be extrapolated to the limit of $L \rightarrow \infty$. For an illustration, the monomer model ($L = 1$) and two polymer models ($L = 3, 4$) of polyethylene glycol are shown in Figure 3a.

The second step was designed to identify possible ensembles of configurational microstates corresponding to each of the (monomer and polymer) models. The procedure involved some substeps. First, starting from an atomic configuration, shown as an orange star in Figure 3b, a molecular dynamics (MD) simulation using an empirical Reax force field³⁷ was performed using Large-scale Atomic/Molecular Massively Parallel Simulator (LAMMPS),³⁸ thoroughly exploring the configuration space while preserving the atomic connectivity.

Along the trajectory, which lasts at least 1 ns, a large number (e.g., thousands) of new atomic configurations (snapshots) was obtained, shown as light-blue circles in Figure 3b. Then the accessible space is sampled by down-selecting these snapshots to a handful set of maximally diversified configurations, represented by red circles in Figure 3b. This selection process involves fingerprinting these snapshots using the Smooth Overlap of Atomic Positions (SOAP) feature^{39,40} and then selecting a given number of candidates that maximize the total pairwise distance among them in the SOAP feature space. Finally, a room-temperature *ab initio* MD simulation was performed for each of the maximally diversified configurations obtained. The goal of this substep was to equilibrate and propagate these configurations, which were prepared using an empirical potential,³⁷ at the first-principles level of energy computations. Each trajectory, lasting at least 1 ps, the typical time scale for atomic relaxation,² is expected to contain an ensemble of microstates corresponding to the initial configuration at the selected temperature T . The trajectories obtained for the set of maximally diversified configurations are depicted in Figure 3b.

In the last step, ΔH^{ROP} is computed from the MD trajectories obtained. Among them, the lowest one, that is, whose averaged potential energy E at equilibration is lowest, is selected. Then the finite-size (L -dependent) estimation of ΔH^{ROP} is computed as

$$\Delta H_L^{\text{ROP}} = \frac{1}{L} \langle E_L \rangle - \langle E_1 \rangle \quad (1)$$

Here, E_L and E_1 are the potential energies at equilibration of the *ab initio* MD trajectories of the polymer model ($L > 1$) and monomer model ($L = 1$), respectively, while $\langle \dots \rangle$ stands for the average over the microstates after equilibration. Given that we have ΔH_L^{ROP} for multiple finite values of L (in this work, we used 3, 4, 5, 6, and for some cases, 16), ΔH^{ROP} is defined as the $L \rightarrow \infty$ (or, equivalently, $1/L \rightarrow 0$) limit of ΔH_L^{ROP} :

$$\Delta H_L^{\text{ROP}} \equiv \lim_{L \rightarrow \infty} \Delta H_L^{\text{ROP}} \quad (2)$$

In practice, ΔH_L^{ROP} values are fitted to a linear function of $1/L$, and the y intercept of this fit is taken to be ΔH^{ROP} . The slope of this linear function, as shown in Figure 3c, is a (physical) measure of how rapidly the ring strain can be relaxed when the monomer is opened and a polymer chain is formed. Therefore, it is generally positive, as summarized in the Supporting Information. With this extrapolation procedure, we are able to probe macromolecular length scales, a limit that can not be approached directly, especially using first-principles computations today.

Within our scheme, *ab initio* MD simulations were performed in the second step, that is, “configuration space searching and sampling”, to equilibrate the initial configuration at first-principles level and to capture their microstates at the desired temperature. As all of our models are nonperiodic, we used the Γ -point version of Vienna *Ab initio* Simulation Package (VASP),^{41,42} employing a basis set of plane waves with kinetic energy up to 400 eV to represent the Kohn–Sham orbitals. The ion–electron interactions were computed using the projector augmented wave (PAW) method⁴³ while the exchange–correlation (XC) energies were computed using the generalized gradient approximation Perdew–Burke–Ernzerhof (PBE) functional.⁴⁴

Because the initial configurations of these *ab initio* MD simulations were prepared at the level of an empirical potential, the trajectories must be long enough for adequate equilibration to be achieved. As the atomic relaxation time is of the order of a picosecond,² these MD simulations need roughly 2000 steps to equilibrate (our time step is 0.5 fs). In fact, our *ab initio* MD runs for monomers exceed 10 000 steps, while those for polymers are at least 3000 steps.

The geometrical optimizations needed to reproduce the results of the conventional approach were performed using VASP. For this purpose, we also used the same PAW potential, the PBE XC functional, and the plane-wave energy cutoff of the aforementioned *ab initio* MD simulations. Convergence in optimizing the structures was assumed when the atomic forces became less than 0.01 eV/Å.

We have computed the ΔH^{ROP} of all 42 ROPs in the benchmark set using the conventional approach. For each of them, we opened the monomer and capped it with two end groups obtained from either ethane $\text{CH}_3\text{—CH}_3$, methylamine $\text{CH}_3\text{—NH}_2$, methanol $\text{CH}_3\text{—OH}$, or methanethiol $\text{CH}_3\text{—SH}$ molecule so that the reaction was isodesmic. Then we performed a comprehensive search for the ground-state atomic configurations of the monomer and the polymer, that is, the capped ring-opening monomer. Finally, the obtained structures were fully optimized using DFT computations.

The computed results are summarized in Figure 4, while details can be found in Table 1. Except for cycloalkanes series whose trend of ΔH^{ROP} is captured, this approach hardly works with other classes of polymers. The overall root-mean-square error (RMSE) of this approach across the benchmark set is roughly 15.4 kJ/mol and the overall coefficient of determination R^2 is 0.75. However, the prediction in the regime between −20 and 0 kJ/mol, which is critical for the purpose of designing depolymerizable polymers, is poor. In particular, the obtained RMSE in this regime is ≈ 19.0 kJ/mol, while for the class of thiolactones, this error is ≈ 23.3 kJ/mol. Such an uncertainty is too large and cannot be used to guide the design of depolymerizable polymers.

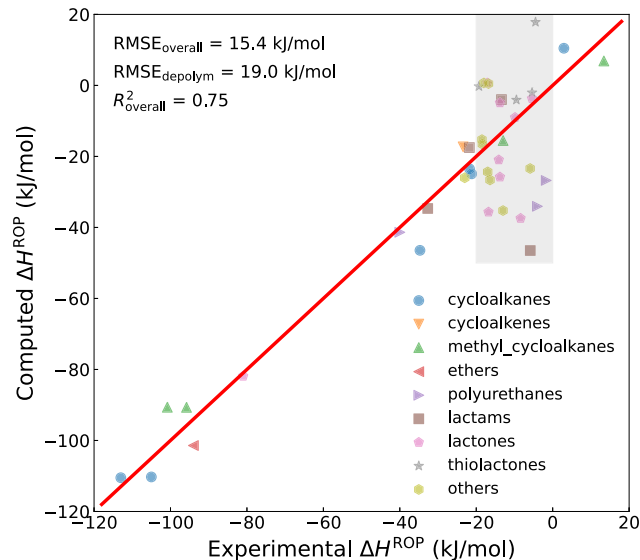


Figure 4. Computed ΔH^{ROP} for the benchmark set of 42 ring-opening polymerization summarized in Figure 2 using past approach. The area of interest for depolymerizable polymers, for which ΔH^{ROP} ranges from −20 to 0 kJ/mol, is shaded. Within this regime, $\text{RMSE}_{\text{depolym}} \approx 19.0$ kJ/mol, while for the whole benchmark set, the obtained $\text{RMSE} \approx 15.4$ kJ/mol.

Table 1. Three Error Measures of Past Approach and Our Approach Including (i) RMSE (kJ/mol), (ii) Relative RMSE, Defined as RMSE Divided by Range of Experimental ΔH^{ROP} , and (iii) Mean Relative Error (MRE)^a

monomer class	past approach			our approach		
	RMSE	relative RMSE	MRE	RMSE	relative RMSE	MRE
cycloalkanes	6.4	0.055	0.54	7.9	0.068	0.37
cycloalkenes	6.1	N/A	0.26	9.7	N/A	0.42
methyl cycloalkanes	6.7	0.059	0.21	8.5	0.074	0.27
ethers	7.4	N/A	0.08	6.2	N/A	0.07
polyurethanes	22.6	0.590	7.43	13.4	0.351	4.78
lactams	21.0	0.782	1.97	5.2	0.195	0.38
lactones	14.1	0.187	0.89	6.1	0.080	0.48
thiolactones	23.3	1.575	2.26	3.6	0.245	0.47
others	13.46	0.912	0.78	6.74	0.396	0.394
overall	15.39	0.122	1.48	7.32	0.058	0.71

^aRelative RMSE is not available (N/A) for monomer classes having one experimental ΔH^{ROP} data point.

We now demonstrate our new scheme to compute ΔH^{ROP} for the benchmark set. For each of the 42 ROPs, monomer and polymer models were created, the corresponding configuration spaces were explored and sampled for computing ΔH_L^{ROP} , and finally they were extrapolated to the limit of $L \rightarrow \infty$ to determine ΔH^{ROP} . In Figure 5a, we illustrate the extrapolation procedure performed on four representative polymers including one lactam, one cycloalkane, one lactone, and one thiolactone. Table 1 provides a comprehensive assessment on the performance of our approach in comparison with the past approach. Three measures of errors are given including (ii) RMSE, (ii) relative RMSE, which is defined as the ratio between RMSE and the actual range of the reference data, that is, experimental ΔH^{ROP} , and (iii) mean relative error (MRE). The full set of 42 extrapolated ΔH^{ROP} are directly compared

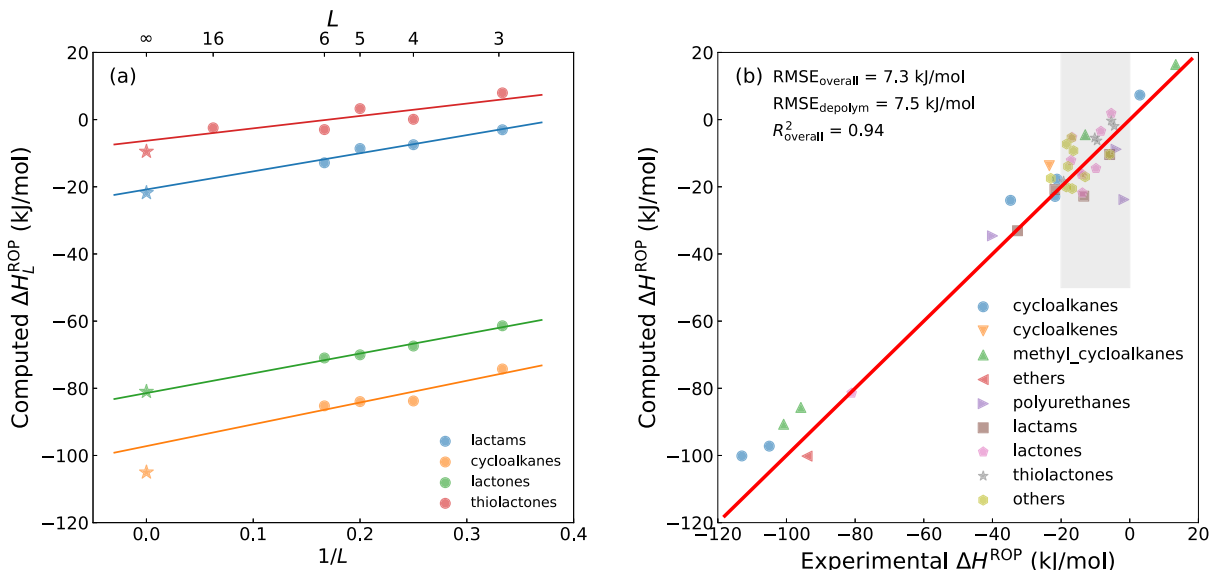


Figure 5. (a) Extrapolation procedure used to find ΔH^{ROP} of four representative polymers including one lactam, one cycloalkane, one lactone, and one thiolactone. For each of them, ΔH_L^{ROP} (solid circles) values are fitted into a linear function of $1/L$ (solid lines), while experimental data are given in stars. (b) Computed ΔH^{ROP} values are given in a comparison with experimental ΔH^{ROP} , in which the RMSE is 7.3 kJ/mol and $R^2 = 0.94$. Within the regime between -20 and 0 kJ/mol (shaded area), RMSE is 7.5 kJ/mol.

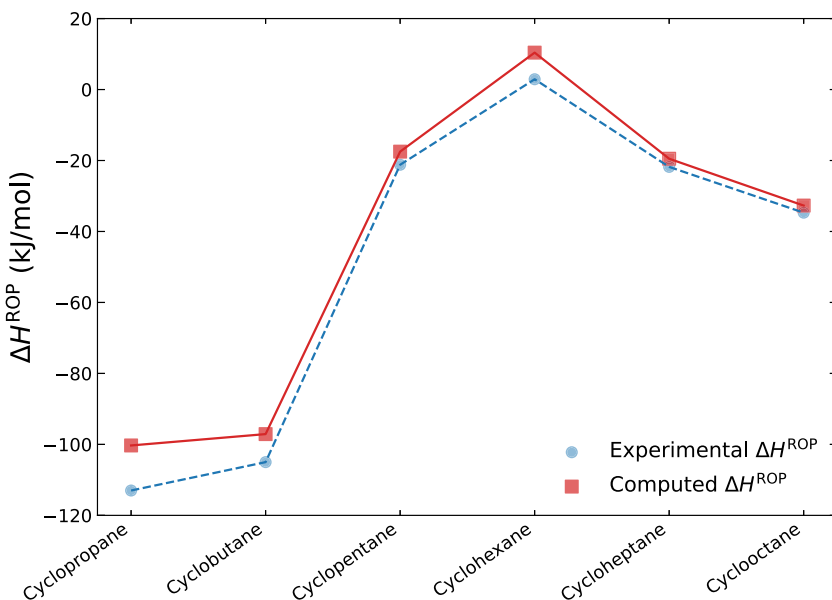


Figure 6. Experimental and computed ΔH for six cycloalkanes with ring size of 3 (cyclopropane), 4 (cyclobutane), 5 (cyclopentane), 6 (cyclohexane), 7 (cycloheptane), and 8 (cyclooctane). Data points are given by symbols, while lines are for a guide of the trend.

with experimental ΔH^{ROP} in Figure 5b and Table 1. Detailed information on the benchmark set including the monomer and polymer SMILES (simplified molecular-input line-entry system)⁴⁵ and the measured and computed ΔH^{ROP} can be found in the Supporting Information.

Figure 5a clearly shows that the finite-size effects, indicated by the slope of the linear fitted lines, are significant. For most of the polymers in the benchmark set, their $L = 6$ models contain roughly 100–200 atoms and more. Even with such a large model, the computed ΔH_L^{ROP} could still be about 10–20 kJ/mol from the experimental value of ΔH^{ROP} . Still, the extrapolation procedure, which assumes a linear dependence of ΔH_L^{ROP} on $1/L$, appears reasonable.

In fact, considering that the benchmark set is extremely diverse and that ΔH^{ROP} is scattered in a wide range (≈ 130 kJ/mol), an RMSE of 7.3 kJ/mol, an R^2 coefficient of 0.94, and detailed results shown in Table 1 demonstrate the robustness of the whole scheme in computing ΔH^{ROP} . Within the benchmark set, the performance of this scheme could be different for different classes, typically with different chemistries. The most probable reason is that configuration space searching and sampling is more efficient for polymers that have no side chains and all rotatable bonds. Rigid bonds in the monomer rings or (large) side chains will certainly make the exploration much more challenging; thus, the configurations selected and used for the *ab initio* MD simulations in such cases may not be good representatives. Moreover, the

experimental values of ΔH^{ROP} in the benchmark set were measured under different conditions using different methods, for example, semiempirical, calorimetry, and NMR spectroscopy. We anticipate that this diversity could play a role in the relatively large errors associated with the predictions for polyurethanes,⁴⁶ that is, $\approx 13.4 \text{ kJ/mol}$, for which the calorimetry method was used. On the other hand, the error for thiolactones, whose ΔH^{ROP} was measured using the NMR spectroscopy,³¹ is $\approx 3.6 \text{ kJ/mol}$, about one order smaller than the error of $\approx 23.3 \text{ kJ/mol}$ when the past approach is used. In the regime of interest pertaining to depolymerizable polymers, the obtained RMSE is $\approx 7.5 \text{ kJ/mol}$, about 3-times smaller than the past approach.

As previously mentioned, the monomer ring size is an important degree of freedom in controlling ΔH^{ROP} . We show in Figure 6 the experimental and computed ΔH^{ROP} of six smallest cycloalkanes with ring size of 3, 4, 5, 6, 7, and 8. Because there are enormous strains in the monomers with small ring size (3 and 4), they are easier to break and polymerize with highly negative $\Delta H^{\text{ROP}} \gtrsim -100 \text{ kJ/mol}$. For medium ring-size monomers (5, 6, and 7), ΔH^{ROP} is less negative and even slightly positive, while ΔH^{ROP} slowly decreases for larger monomers. Over a very large range of values (from -100 to 3 kJ/mol), our computed ΔH^{ROP} closely follows this trend with an RMSE $\approx 8 \text{ kJ/mol}$, that is, about 10% of the range.

The trend shown in Figure 6 with respect to the monomer ring size for the series of cycloalkanes is quite general and resembles that for other classes of polymers as well. Overall, small ring-size monomers are highly unstable and can easily be polymerized, that is, depolymerizations are difficult. Monomers in which five-, six- and seven-membered rings are opened will be more relevant for the goal of designing depolymerizable polymers. The reason is that for these monomers, ΔH^{ROP} are slightly negative, and thus, while polymerization will be thermodynamically favored at low temperatures, depolymerization may be accomplished at moderate temperatures.

Within the benchmark set, the series of thiolactones were developed by us.³¹ Each monomer in this series contains one six-membered ring with one or two sulfur atoms. Because S–C bonds ($\approx 1.8\text{--}1.9 \text{ \AA}$) are typically about 20–30% longer than C–C bonds ($\approx 1.4\text{--}1.5 \text{ \AA}$), thiolactones may face more ring strain than the six-membered ring monomer of cycloalkanes, that is, cyclohexane. On the other hand, the strain in thiolactones is still much less than cyclopentane (five-membered ring) and cyclobutane (four-membered ring) in which the bond angle of the sp^3 carbon atoms is significantly deformed from 120 degrees to ≈ 106 degrees and ≈ 90 deg, respectively. Consequently, ΔH^{ROP} of thiolactones is in the range between ~ -10 and $\approx 0 \text{ kJ/mol}$ (compared to -81.0 kJ/mol of cyclobutane, -21.2 kJ/mol of cyclopentane and 2.9 kJ/mol of cyclohexane), and polymers in this classes are good candidates for depolymerizable polymers. As shown in Figure 5, our computational scheme is accurate for thiolactones with an RMSE of 3.6 kJ/mol in predicting ΔH^{ROP} .

Ring-opening polymerization enthalpy ΔH^{ROP} is a critical concept for rationally exploring the polymer space and designing depolymerizable polymers. Of note, computing ΔH^{ROP} in a reliable and accurate manner is nontrivial. Here, we have developed a first-principles scheme capable of high-fidelity computations of ΔH^{ROP} with an averaged error of about 7 kJ/mol across a highly diverse benchmark set of 42 ROPs, and an average of about 3.6 kJ/mol for chemical classes

such as thiolactones, which are most suitable for this space of recyclable polymers. This accurate scheme may thus be used to guide the design of depolymerizable polymers.

While multiple challenges in computing ΔH^{ROP} , for example, the finite-size effects, the end-cap effects, and the single-configuration approximation, were resolved, other problems, including effects of solvent and entropic contributions to the Gibbs free energy, remain open. Moreover, this scheme is computationally very demanding, and further developments of this scheme would be needed to address these deficiencies. As the DFT-based molecular dynamics simulations in the second step are the main bottleneck, they are needed to reach the accuracy required in computing ΔH^{ROP} . Faster potentials such as reaxFF or machine-learning force fields can easily be used in this scheme when their accuracy and transferability are secured. Given that a high-quality data set of ROPs and computed ΔH^{ROP} has been developed (and can be scaled up), machine-learning (ML) methods may be used in multiple ways, including (i) extracting important features that control ΔH^{ROP} , (ii) building ML models to instantaneously predict ΔH^{ROP} , and (iii) planning the computations of ΔH^{ROP} in an efficient and on-demand manner, ultimately accelerating the design of depolymerizable polymers with suitable T_c and other desired properties.

ASSOCIATED CONTENT

Supporting Information

The Supporting Information is available free of charge at <https://pubs.acs.org/doi/10.1021/acs.jpcllett.2c00995>.

Detailed information on benchmark set of 42 polymers, including monomer SMILES, polymer SMILES, experimental ΔH^{ROP} , computed ΔH^{ROP} , and slope obtained from extrapolation step of our scheme (PDF)

AUTHOR INFORMATION

Corresponding Author

Rampi Ramprasad – School of Materials Science and Engineering, Georgia Institute of Technology, Atlanta, Georgia 30332, United States;  orcid.org/0000-0003-4630-1565; Email: rampi.ramprasad@mse.gatech.edu

Authors

Huan Tran – School of Materials Science and Engineering, Georgia Institute of Technology, Atlanta, Georgia 30332, United States;  orcid.org/0000-0002-8093-9426

Aubrey Toland – School of Materials Science and Engineering, Georgia Institute of Technology, Atlanta, Georgia 30332, United States

Kellie Stellmach – School of Chemistry and Biochemistry, Georgia Institute of Technology, Atlanta, Georgia 30332, United States

McKinley K. Paul – School of Chemistry and Biochemistry, Georgia Institute of Technology, Atlanta, Georgia 30332, United States

Will Gutekunst – School of Chemistry and Biochemistry, Georgia Institute of Technology, Atlanta, Georgia 30332, United States;  orcid.org/0000-0002-2427-4431

Complete contact information is available at:

<https://pubs.acs.org/10.1021/acs.jpcllett.2c00995>

Notes

The authors declare no competing financial interest.

Data from this work can be found in the Supporting Information and at <https://khazana.gatech.edu/>.

ACKNOWLEDGMENTS

The authors are grateful for the financial support from the Office of Naval Research through a Multidisciplinary University Research Initiative (MURI) Grant (N00014-20-1-2586). They also thank Harikrishna Sahu for technical help and XSEDE for computational support through allocation DMR080044.

REFERENCES

- (1) Young, R. J.; Lovell, P. A. *Introduction to polymers*; CRC Press, 2011.
- (2) Huan, T. D.; Boggs, S.; Teyssedre, G.; Laurent, C.; Cakmak, M.; Kumar, S.; Ramprasad, R. Advanced polymeric dielectrics for high energy density applications. *Prog. Mater. Sci.* **2016**, *83*, 236.
- (3) U.S. Environmental Protection Agency. *Facts and Figures about Materials, Waste and Recycling - Plastics: Material-Specific Data*; U.S. EPA, 2021. <https://www.epa.gov/facts-and-figures-about-materials-waste-and-recycling/plastics-material-specific-data> (accessed 01-21-2022).
- (4) Borrelle, S. B.; et al. Predicted growth in plastic waste exceeds efforts to mitigate plastic pollution. *Science* **2020**, *369*, 1515–1518.
- (5) Rochman, C. M.; Browne, M. A.; Halpern, B. S.; Hentschel, B. T.; Hoh, E.; Karapanagioti, H. K.; Rios-Mendoza, L. M.; Takada, H.; Teh, S.; Thompson, R. C. Classify plastic waste as hazardous. *Nature* **2013**, *494*, 169–171.
- (6) Jambeck, J. R.; Geyer, R.; Wilcox, C.; Siegler, T. R.; Perryman, M.; Andrady, A.; Narayan, R.; Law, K. L. Plastic waste inputs from land into the ocean. *Science* **2015**, *347*, 768–771.
- (7) Hamad, K.; Kaseem, M.; Deri, F. Recycling of waste from polymer materials: An overview of the recent works. *Polym. Degrad. Stab.* **2013**, *98*, 2801–2812.
- (8) Coates, G. W.; Getzler, Y. D. Chemical recycling to monomer for an ideal, circular polymer economy. *Nat. Rev. Mater.* **2020**, *5*, 501–516.
- (9) Lange, J.-P. Sustainable development: efficiency and recycling in chemicals manufacturing. *Green Chem.* **2002**, *4*, 546–550.
- (10) Lange, J.-P. Managing plastic waste- sorting, recycling, disposal, and product redesign. *ACS Sustain. Chem. Eng.* **2021**, *9*, 15722–15738.
- (11) Schyns, Z. O.; Shaver, M. P. Mechanical recycling of packaging plastics: A review. *Macromol. Rapid Commun.* **2021**, *42*, 2000415.
- (12) Shams, M.; Alam, I.; Mahbub, M. S. Plastic pollution during covid-19: Plastic waste directives and its long-term impact on the environment. *Environ. Adv.* **2021**, *5*, 100119.
- (13) Tardy, A.; Nicolas, J.; Gigmes, D.; Lefay, C.; Guillaneuf, Y. Radical ring-opening polymerization: scope, limitations, and application to (bio) degradable materials. *Chem. Rev.* **2017**, *117*, 1319–1406.
- (14) Hong, M.; Chen, E. Y.-X. Completely recyclable biopolymers with linear and cyclic topologies via ring-opening polymerization of γ -butyrolactone. *Nat. Chem.* **2016**, *8*, 42–49.
- (15) Olsén, P.; Odelius, K.; Albertsson, A.-C. Thermodynamic presynthetic considerations for ring-opening polymerization. *Biomacromolecules* **2016**, *17*, 699–709.
- (16) Dubois, P.; Coulembier, O.; Raquez, J.-M. *Handbook of ring-opening polymerization*; Wiley Online Library, 2009.
- (17) Russo, S.; Casazza, E. *Polymer science: A comprehensive reference*; Matyjaszewski, K., Möller, M., Eds.; Elsevier: Amsterdam, 2012; pp 331–396.
- (18) Greer, S. C. Physical chemistry of equilibrium polymerization. *J. Phys. Chem. B* **1998**, *102*, 5413–5422.
- (19) Dainton, F.; Ivin, K. Reversibility of the propagation reaction in polymerization processes and its manifestation in the phenomenon of a “ceiling temperature. *Nature* **1948**, *162*, 705–707.
- (20) Duda, A.; Kowalski, A. *Handbook of ring-opening polymerization*; Dubois, P., Coulembier, O., Raquez, J.-M., Eds.; Wiley Online Library: Oxford, 2009; Chapter 1, pp 1–51.
- (21) Pearce, A. K.; Foster, J. C.; O'Reilly, R. K. Recent developments in entropy-driven ring-opening metathesis polymerization: Mechanistic considerations, unique functionality, and sequence control. *J. Polym. Sci. A: Polym. Chem.* **2019**, *57*, 1621–1634.
- (22) Dudev, T.; Lim, C. Ring strain energies from ab initio calculations. *J. Am. Chem. Soc.* **1998**, *120*, 4450–4458.
- (23) Katiyar, V.; Nanavati, H. Ring-opening polymerization of l-lactide using n-heterocyclic molecules: mechanistic, kinetics and dft studies. *Polym. Chem.* **2010**, *1*, 1491–1500.
- (24) Del Rosal, I.; Poteau, R.; Maron, L. DFT study of the ring opening polymerization of ϵ -caprolactone by grafted lanthanide complexes: 1-effect of the grafting mode on the reactivity of borohydride complexes. *Dalton Trans.* **2011**, *40*, 11211–11227.
- (25) Blake, T. R.; Waymouth, R. M. Organocatalytic ring-opening polymerization of morpholinones: New strategies to functionalized polyesters. *J. Am. Chem. Soc.* **2014**, *136*, 9252–9255.
- (26) Wang, Y.; Li, M.; Chen, J.; Tao, Y.; Wang, X. O-to-s substitution enables dovetailing conflicting cyclizability, polymerizability, and recyclability: dithiolactone vs. dilactone. *Angew. Chem., Int. Ed.* **2021**, *133*, 22721–22727.
- (27) Zhu, N.; Liu, Y.; Liu, J.; Ling, J.; Hu, X.; Huang, W.; Feng, W.; Guo, K. Organocatalyzed chemoselective ring-opening polymerizations. *Sci. Rep.* **2018**, *8*, 1–8.
- (28) Hohenberg, P.; Kohn, W. Inhomogeneous electron gas. *Phys. Rev.* **1964**, *136*, B864–B871.
- (29) Kohn, W.; Sham, L. Self-consistent equations including exchange and correlation effects. *Phys. Rev.* **1965**, *140*, A1133–A1138.
- (30) Overberger, C. G.; Weise, J. K. Anionic ring-opening polymerization of thiolactones. *J. Am. Chem. Soc.* **1968**, *90*, 3533–3537.
- (31) Stellmach, K. A.; Paul, M. K.; Xu, M.; Su, Y.-L.; Fu, L.; Toland, A. R.; Tran, H.; Chen, L.; Ramprasad, R.; Gutekunst, W. R. *Modulating polymerization thermodynamics of thiolactones through substituent and heteroatom incorporation*, submitted 2022.
- (32) Bash, P. A.; Ho, L. L.; MacKerell, A. D.; Levine, D.; Hallstrom, P. Progress toward chemical accuracy in the computer simulation of condensed phase reactions. *Proc. Natl. Acad. Sci. U.S.A.* **1996**, *93*, 3698–3703.
- (33) Dasgupta, S.; Lambros, E.; Perdew, J. P.; Paesani, F. Elevating density functional theory to chemical accuracy for water simulations through a density-corrected many-body formalism. *Nat. Commun.* **2021**, *12*, 1–12.
- (34) Trushin, E.; Thierbach, A.; Görling, A. Toward chemical accuracy at low computational cost: Density-functional theory with σ -functionals for the correlation energy. *J. Chem. Phys.* **2021**, *154*, 014104.
- (35) Huan, T. D.; Ramprasad, R. Polymer structure predictions from first principles. *J. Phys. Chem. Lett.* **2020**, *11*, 5823–5829.
- (36) Sahu, H.; Shen, K.-H.; Montoya, J.; Tran, H.; Ramprasad, R. Polymer structure predictor (psp): a python toolkit for predicting atomic-level structural models for a range of polymer geometries. *J. Chem. Theory Comput.* **2022**, *18*, 2737–2748.
- (37) Wood, M. A.; Van Duin, A. C.; Strachan, A. Coupled thermal and electromagnetic induced decomposition in the molecular explosive α hxmx; a reactive molecular dynamics study. *J. Phys. Chem. A* **2014**, *118*, 885–895.
- (38) Plimpton, S. Fast parallel algorithms for short-range molecular dynamics. *J. Comput. Phys.* **1995**, *117*, 1–19.
- (39) De, S.; Bartók, A. P.; Csányi, G.; Ceriotti, M. Comparing molecules and solids across structural and alchemical space. *Phys. Chem. Chem. Phys.* **2016**, *18*, 13754–13769.
- (40) Himanen, L.; Jäger, M. O. J.; Morooka, E. V.; Federici Canova, F.; Ranawat, Y. S.; Gao, D. Z.; Rinke, P.; Foster, A. S. Dscribe: Library of descriptors for machine learning in materials science. *Comput. Phys. Commun.* **2020**, *247*, 106949.

- (41) Kresse, G.; Furthmüller, J. Efficiency of ab-initio total energy calculations for metals and semiconductors using a plane-wave basis set. *Comput. Mater. Sci.* **1996**, *6*, 15–50.
- (42) Kresse, G.; Furthmüller, J. Efficient iterative schemes for ab initio total-energy calculations using a plane-wave basis set. *Phys. Rev. B* **1996**, *54*, 11169–11186.
- (43) Blöchl, P. E. Projector augmented-wave method. *Phys. Rev. B* **1994**, *50*, 17953–17979.
- (44) Perdew, J. P.; Burke, K.; Ernzerhof, M. Generalized gradient approximation made simple. *Phys. Rev. Lett.* **1996**, *77*, 3865–3868.
- (45) Weininger, D. SMILES, a chemical language and information system. 1. Introduction to methodology and encoding rules. *J. Chem. Inf. Comput. Sci.* **1988**, *28*, 31–36.
- (46) Lebedev, B.; Veridusova, V.; Höcker, H.; Keul, H. Thermodynamics of aliphatic cyclic urethanes, of their ring-opening polymerization, and of corresponding polyurethanes. *Macromol. Chem. Phys.* **2002**, *203*, 1114–1125.

□ Recommended by ACS

Sequential Polymerization from Complex Monomer Mixtures: Access to Multiblock Copolymers with Adjustable Sequence, Topology, and Gradient Strength

Xiaochao Xia, Toshifumi Satoh, *et al.*

DECEMBER 28, 2022

MACROMOLECULES

READ ▶

Sequence-Enhanced Self-Healing in “Lock-and-Key” Copolymers

Yuqi Zhao, Michael R. Bockstaller, *et al.*

MARCH 27, 2023

ACS MACRO LETTERS

READ ▶

Stochastic and Deterministic Analysis of Reactivity Ratios in the Partially Reversible Copolymerization of Lactide and Glycolide

Louise Kuehster, Nathaniel A. Lynd, *et al.*

AUGUST 11, 2022

MACROMOLECULES

READ ▶

Canonicalizing BigSMILES for Polymers with Defined Backbones

Tzyy-Shyang Lin, Bradley D. Olsen, *et al.*

OCTOBER 14, 2022

ACS POLYMERS AU

READ ▶

[Get More Suggestions >](#)